A simple configuration for fabrication of 2D and 3D photonic quasicrystals with complex structures

XiaoHong Sun[1]*, Shuai Wang[1], Wei Liu[1], and LiuDi Jiang[2]

[1]Henan Key Laboratory of Laser and Opto-electric Information Technology, School of Information Engineering, Zhengzhou University, Henan 450052, P. R. China

[2]Faculty of Engineering and the Environment, University of Southampton, UK

*Corresponding email: iexhsun@zzu.edu.cn

Abstract: A simple method using a single-prism common-path interferometer is presented for the fabrication of complex quasicrystals in sub-micrometer scales. Multiple types of two-dimensional (2D) and three-dimensional (3D) quasicrystalline structures are designed and their diffraction patterns are obtained by using Fourier Transform method. Multi-fold rotational symmetries are demonstrated and compared. By using this method, a wide range of quasicrystals types can be produced with arbitrary complexities and rotational symmetries. The transmittance studies of 12-fold and 18-fold structures also reveal the existence of complete photonic bandgaps, which also demonstrates increased symmetry and significantly improved characteristics of photonic band-gaps.

Key words: photonic quasicrystals; top-cut prism; common-path interferometer

1. Introduction

Photonic quasicrystals (PQCs) have attracted significant interest in recent years because they exhibit superior performance as in comparison with periodic photonic crystals (PhC) [1-3]. For example, a PQC can exhibit a complete Photonic Band Gap (PBG) with low refractive index contrast [4] and independence of direction, rich

defect mode, etc. With the increase of rotational symmetry of PQCs, the photonic band becomes more circular in 2D (or spherical in 3D), which greatly increases the possibility of a complete bandgap generation [5-6]. Higher-dimensional photonic quasicrystals (2D and 3D) offer greater flexibility over 1D structures in the design of their geometry and potential applications. However, the design rules become increasingly complex as one considers the broader range of deterministic aperiodic structures. This is demonstrated by the fact that tiling rules for 2D quasicrystals do not exist for geometries that exhibit more than 14-fold rotational symmetry [7]. On the other hand, large area production of quasicrystalline structures is extremely challenging using conventional micro/nano fabrication processes [8-10]. Hence, a simple and effective method is required to realize the design and fabrication of complex quasicrystals with higher symmetry and dimensions.

Laser holographic lithography has been recently reported to realize PBG materials [11, 12]. In principle, multi-beam laser interference is exploited to form holographic patterns in space which subsequently expose a photosensitive medium to form designed patterns. Lattice constant and structure of PGB materials can be tuned and fabricated in a flexible manner. Among these laser lithography technologies, it is known that the single diffraction [13] or refraction element [14-19] method is the most encouraging as it is suitable for large-area manufacturing. Nonetheless, in our previous studies of PBG structures [16-19], we found that a specific type of prism only corresponds to a specific type of quasicrystalline structure. For instance, a pentagonal prism only leads to ten-fold quasicrystals. This suggests that the ever increasing demand of PQC with high symmetries and complexities would largely rely on the design and manufacture of complex prisms, which may be practically difficult and costly. The usage of complex prism will also significantly complicate the potential optical path adjustment and large area of crystal fabrications.

A single-prism system, combined with sample rotation and multiple exposures, is reported in this work to fabricate 2D and 3D complex PQC structures. The experimental setup is simple, easy to adjust and potentially suitable for large-area

fabrication of PQCs in sub-micrometer scales. A high level of schematic stability is also observed due to common path interference. In addition, the transmittance of a 12-fold and an 18-fold PQCs is calculated and compared to characterize their photonic band-gaps of transverse electric (TE) and magnetic (TM) modes, respectively.

2. Theoretical modeling of 2D PQC structures

Fig. 1 shows a schematic diagram of the designed setup. An expanded laser beam was incident from top and refracted into two beams for a prism (fig. 1a) or four beams for a Top-Cut Triangular Prism (TCTP, fig. 1b). Subsequently, the refractive beams were combined and interfered after exiting the bottom surface of the prism. The interfering patterns were then recorded on the photosensitive medium. Following the developing process of the exposed medium, the designed PQC structures were obtained. A polarization or phase plate was used to adjust the polarized direction or initial phase of the incident beam. A rotary table was used to regulate the relative position between the medium and prism, which can adjust the rotational symmetry of PQCs.

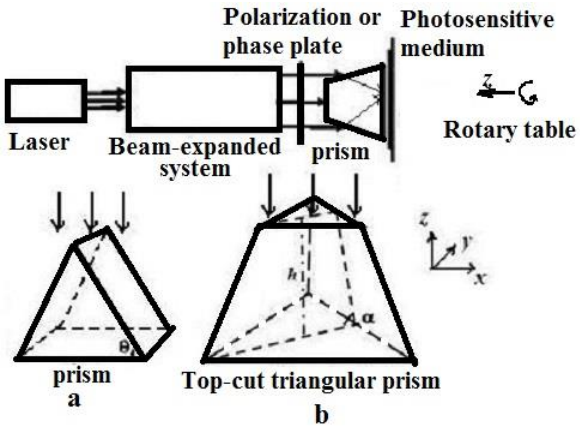

Fig.1 Schematic diagram of single-prism common-path interferometer (a) prism (b) TCTP

Assuming the same polarization and initial phase for the incident beams, the interference intensity on the medium can be expressed as [18]

$$I(r)=\sum_{j,l}E_jE_l^{*}exp\left\{-i\left[(\vec{k}_j-\vec{k}_l)\cdot\vec{r}\right]\right\}\quad,\quad (1)$$

Where E_j is the amplitude of beam j, $\vec{r}=(x,y,z)$ is the spatial position vector.

For the prism system (fig. 1a), j,l=1~2 and thus the wave vectors are

$$\vec{k}_m=k\left(\pm sin\phi,0,cos\phi\right),\quad (2)$$

Where $m=1,2$ is corresponding to the signs "+" and "-", respectively. ϕ is defined as an angle $\phi=\theta-\arcsin\left(\sin\theta/n_w\right)$, where θ is the crossing angle between the side and ground of prism.

For the TCTP system in Fig. 1b, j,l=1~3. If the central beam is blocked, the wave vectors of three side beams are

$$\vec{k}_m=k\left(cos\frac{2(m-1)\pi}{3}sin\varphi,sin\frac{2(m-1)\pi}{3}sin\varphi,cos\varphi\right),\quad (3)$$

Where m=1~3, $\varphi=\alpha-\arcsin\left(\sin\alpha/n_w\right)$ and α is the crossing angle as shown in Fig1b.

In the equation 1~3, $k=2\pi n_w/\lambda$ and n_w is the refractive index of the medium in the writing laser wavelength. Given the parameters of the prism and the beam wavelength, the interferogram corresponding to complex PQCs can be achieved by using the software Matlab2015 and the Equation (1)~(3).

2.1 Design of 2D PQCs using the prism

For the prism system as shown in Fig.1a, substituting $\theta=66^0, n_w=1.5$ and $\lambda=355nm$ into the equations (1) and (2), an interferogram 1 was obtained and shown in Fig.2a. The period of the structure of interferogram 1 is $\Lambda=\lambda/2n_w\sin\phi=248nm$ in the range of the ultraviolet (UV) wavelength. Furthermore, interferograms 2, 3 and 4 were obtained by rotating an angle of π/4, π/2 and 3π/4 from the pattern 1, respectively. An 8-fold PQC was formed by superpositioning interferograms 1~4, as a diagram is shown in Fig. 2b.

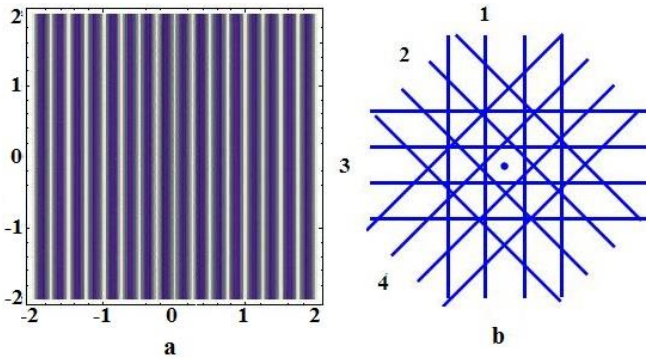

Fig.2 a) two-beam interferogram b) diagram of 8-fold quasicrystal formed by the prism interferometery

Therefore, in principle, 8-fold PQCs can be produced by controlled rotating and then exposing the medium four times, where four groups of Bragg gratings can be recorded. Similarly, a 10-fold PQC could also be obtained by applying rotating angles of $\pi/5$, $2\pi/5$, $3\pi/5$ and $4\pi/5$ and exposing five times, while a 14-fold PQC could be fabricated using rotating angle of $\pi/7$, $2\pi/7$, $3\pi/7$, $4\pi/7$, $5\pi/7$ and $6\pi/7$ with seven times exposures in total. Fig. 3 a-c compares the patterns of 8, 10 and 14 folds PQCs and the insets of the enlarged central patterns clearly show the designed PQCs. Fig.3d-f also shows their corresponding Fourier Transforming patterns, respectively. Thus, we believe PQCs with an arbitrary even rotational symmetry could be obtained using the suggested single prism setup Fig.1a.

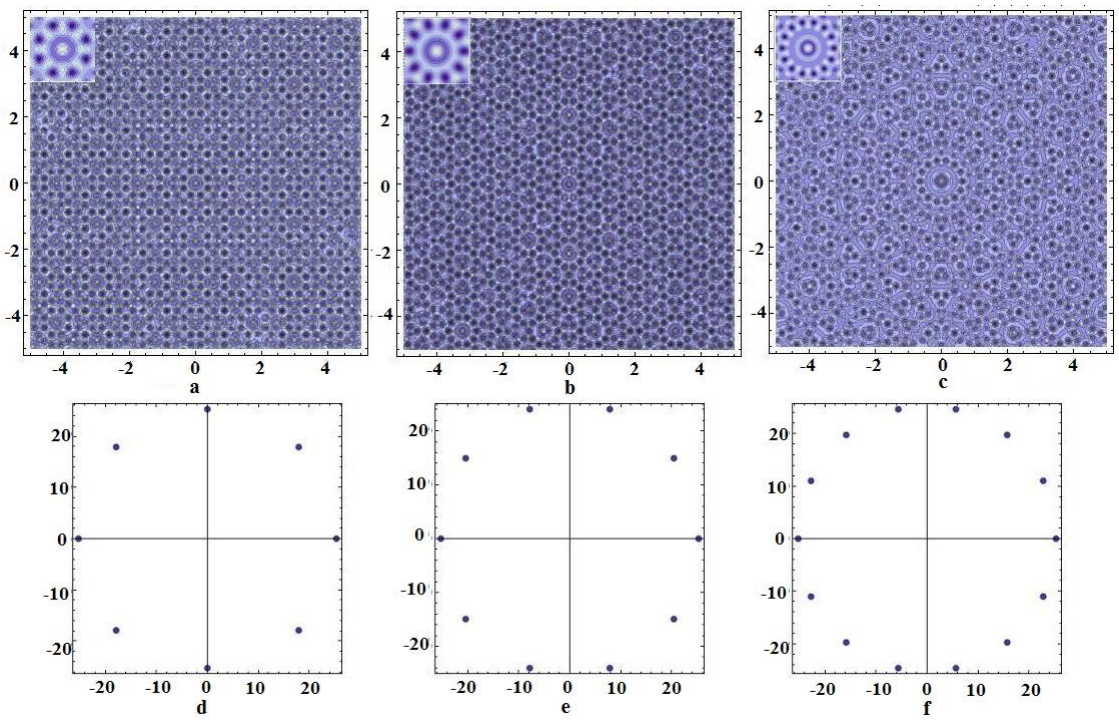

Fig.3 Quasicrystalline structures of a) 8-fold b) 10-fold and c) 14-fold,

the corresponding central area in the inset and Fourier Transform patterns in d), e) and f)

2.2 PQCs designed by using the TCTP

For the TCTP prism system, substitute $\theta = 54.7^0, n_w = 1.5$ and $\lambda = 355\text{nm}$ into equations (1) and (3), a calculated interferogram is shown in Figure4a. This is a periodic PhC structure with hexagonal or triangular lattices and its period is $\Lambda = \lambda/\{n_w[1-\cos(2\pi/3)]\sin\varphi\} = 405nm$ which is also within UV wavelength range. Fig.4a shows that the structure is composed of three groups of interlaced interference planes (black lines) which are formed by any two of the three refracted beams. Fig.4b is a diagram of a 12-fold quasicrystal formed by the superposition of the structure with each component obtained by rotating an angle of a π/6 interval.

Based on the hexagonal structure formed by the TCTP, multi-fold PQCs can be designed and fabricated by controlling the rotational angle and times of exposures for photosensitive medium. We further studied the quantitative relationship between the PQC symmetry and key process parameters. Assuming the exposure times as n (n=1 corresponds to the starting position) and a single rotation angle as $\pi/3n$, the obtained

PQCs have 6n rotational symmetries. For example, a 12-fold PQC corresponds to n=2, and the rotational times and angle are 1 and $\pi/6$, respectively.

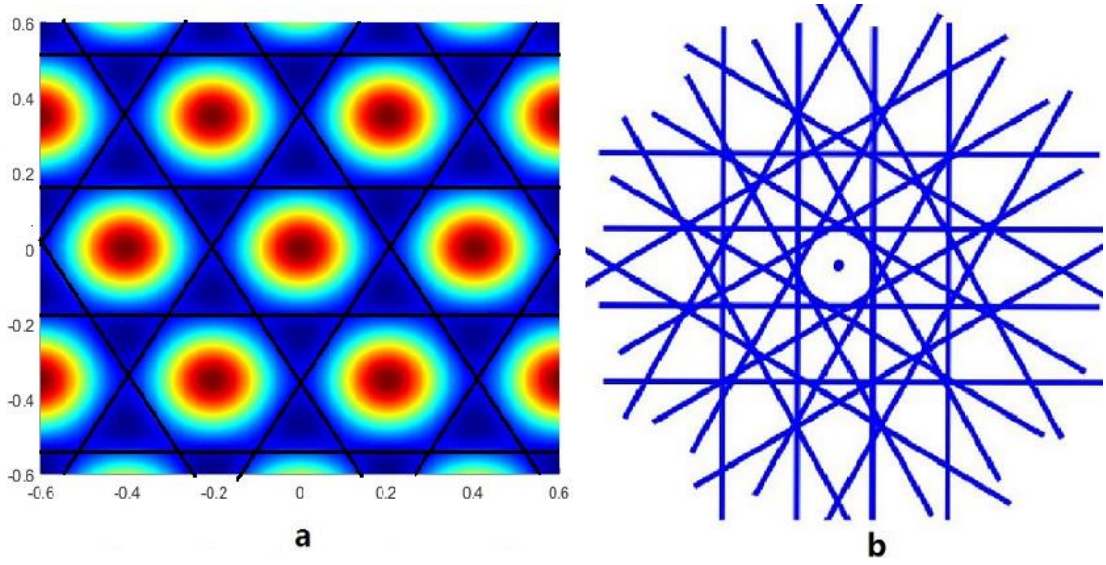

Fig.4 a) three-beam interferogram b) diagram of 12-fold quasicrystal formed by the TCTP interferometer

n=2, 3, 4 correspond to rotation angles of $\pi/6$, $\pi/9$, $\pi/12$, respectively, which lead to PQC structures with 12-fold, 18-fold and 24-fold designs as shown in Fig.5a, b and c, respectively. Fig.5d, e and f show corresponding Fourier Transform patterns. Multiple rotational symmetries of PQCs can thus be generated. Based on this principle, any complex PQCs with 6n rotational symmetries could be produced.

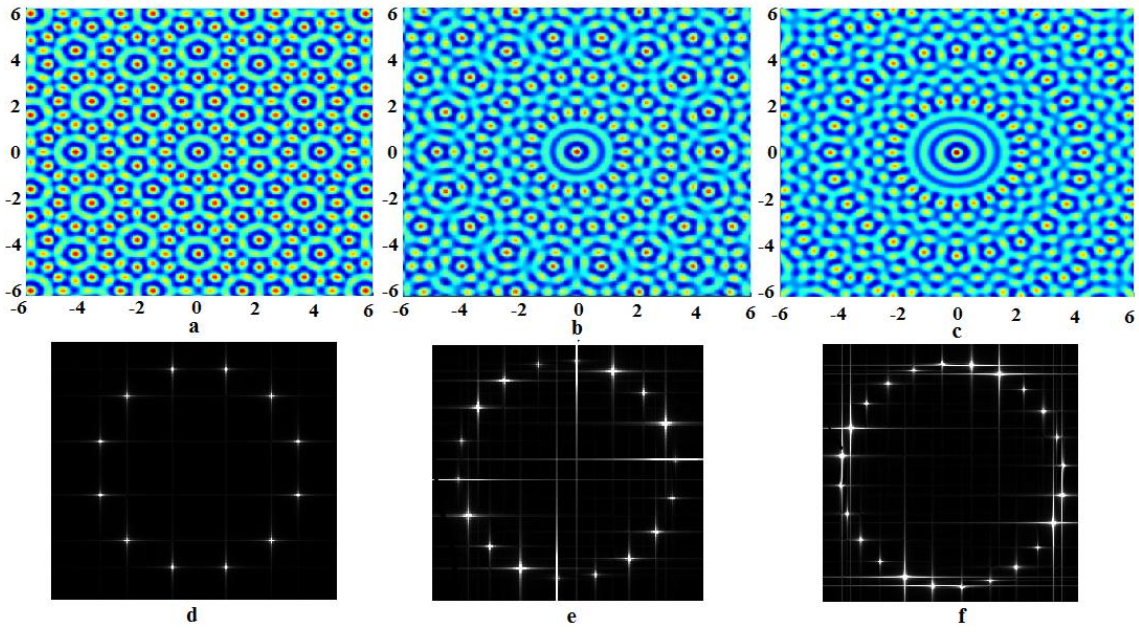

Fig.5 Quasicrystalline structures of a) 12-fold b) 18-fold c) 24-fold,

and Fourier Transform patterns in d), e) and f)

3. Design of 3D multi-fold PQC structures

For the TCTP interferometer in Fig.1b, if the central beam k_0=k(0,0,1) is added to the interfering system, thus j,l=0~3 in the Eq.1, the 3D interfering field can be obtained in Fig.6. Fig.6a, b, c and d reveal a 3D structure and sectional views of *x*-*y* plane, *x*-*z* plane and *y*-*z* plane, respectively. Coordinate system is also shown in the figure. This is a periodical crystal with a complex hexagonal lattice. The structure is composed of two types of rods with different intensities, orange and light blue. In the *x*-*y* plane, hexagonal or triangular lattices and honeycomb lattices are formed by orange rods and light blue rods, respectively. In the *x*-*z* and *y*-*z* planes, rectangular lattices are observed clearly. The lattice constants in *x*, *y* and *z* directions are

$$\Delta x = 2\pi/(k_{1x} - k_{2x}) = \lambda \Big/ \left\{ n_w \left[1 - \cos\left(2\pi/3\right) \right] \sin\varphi \right\} = 405nm$$

$$\Delta y = 2\pi/(k_{1y} - k_{2y}) = \lambda \Big/ \left[n_w \sin\left(2\pi/3\right) \sin\varphi \right] = 702nm$$

$$\Delta z = 2\pi/(k_{0z} - k_{1z}) = \lambda \Big/ \left[n_w \left(1 - \cos\varphi\right) \right] = 2998nm,$$

for the lattices of light blue rods. For the orange rod lattice, the corresponding values are 1216nm, 702nm and 2998nm, respectively.

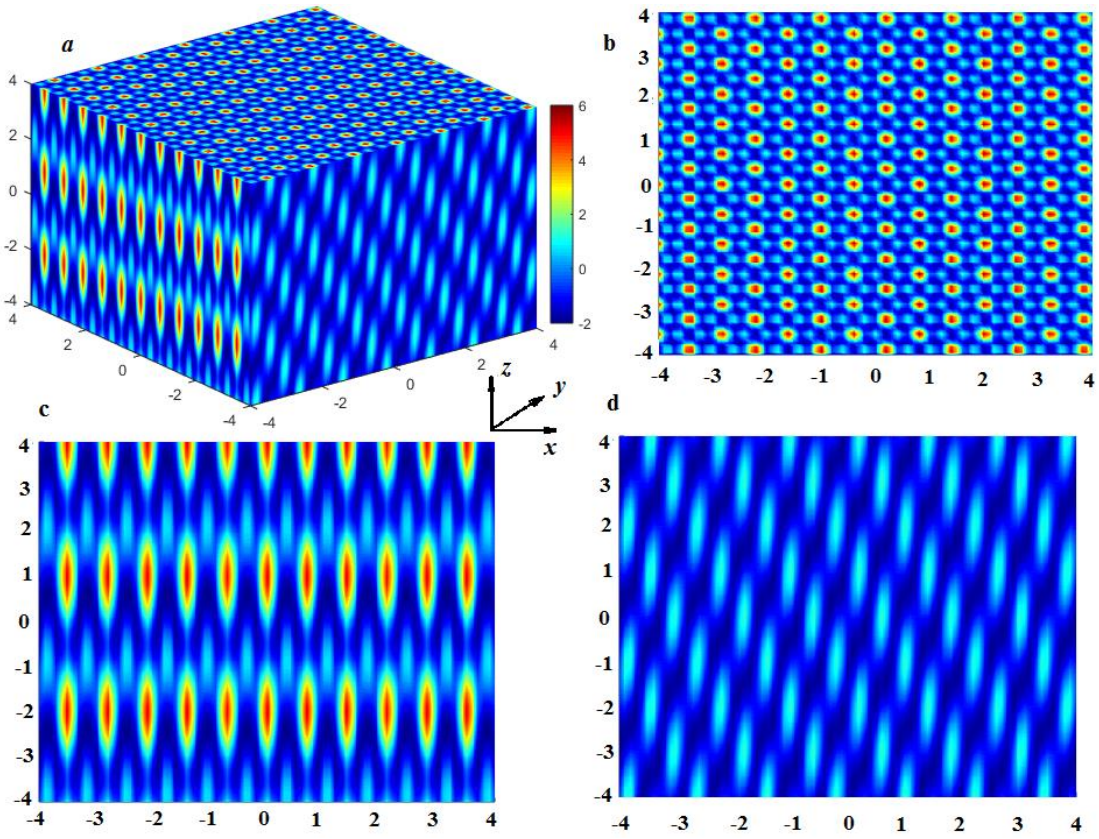

Fig.6 Four beams interfering patterns (a) 3D diagram

(b) *x*-*y* plane pattern (c) *x*-*z* plane pattern (d) *y*-*z* pattern

When the photosensitive medium is rotated an angle π/6 along *z* axis, two 3D structures in the Fig.6a are superposed in the different direction to get a 3D quasicrystalline structure, as shown in Fig.7. It is observed that the structure is composed of a 12-fold rotational symmetrical quasicrystal in *x*-*y* plane and a periodical structure with rectangular lattices in x-z and y-z planes. Fourier transform pattern of the x-y sectional structure is also obtained and shown in Fig.7d. The pattern reveals the existence of 12-fold rotational symmetry more obviously.

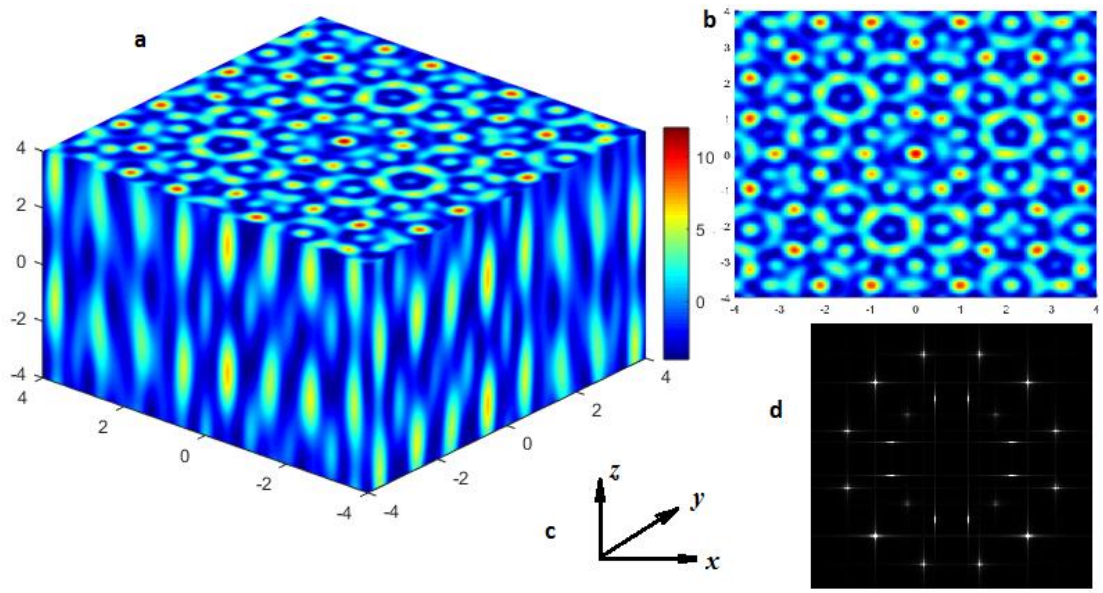

Fig.7 (a) 3D structure of 12-fold quasicrystals (b) *x-y* plane diagram

(c) Coordinate system (d) Fourier transform pattern

In the same way, by rotating an angle of a $\pi/9$ interval two times and an angle of $\pi/12$ three times, 3D 18-fold and 24-fold quasicrystalline structures can be obtained in Fig.8 and Fig.9. Fig.8b and Fig.9b are the views of *x-y* plane and show the 18-fold and 24-fold rotational symmetry, respectively. The Fourier transformation of the *x-y* plane signifies their multi-fold symmetries more clearly. The side views of x-z and y-z planes also manifest the periodical structure with rectangular lattices.

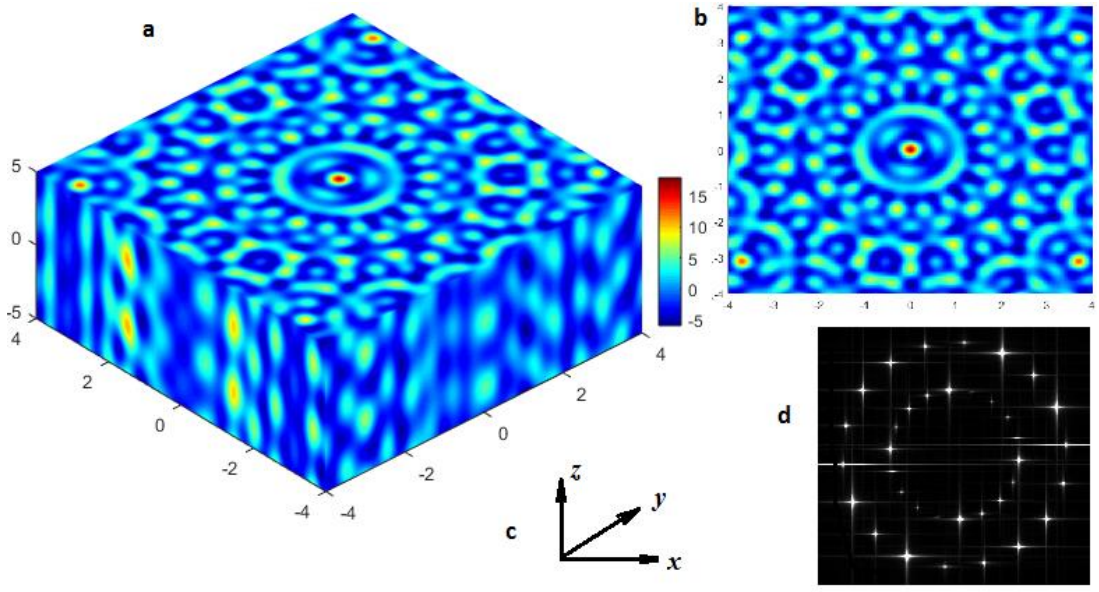

Fig.8 (a) 3D structure of 18-fold quasicrystals (b) *x-y* plane diagram

(c) Coordinate system (d) Fourier transform pattern

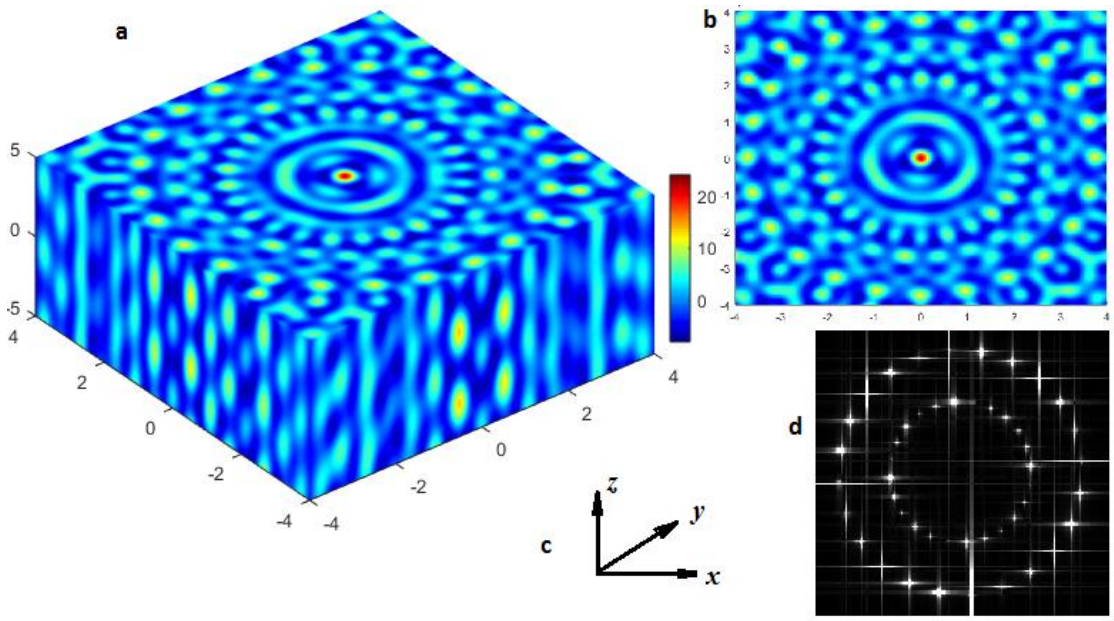

Fig.9 (a) 3D structure of 24-fold quasicrystals (b) *x*-*y* plane diagram

(c) Coordinate system (d) Fourier transform pattern

4. Calculating of photonic bands

The transmission diffraction efficiency was also modeled for 12-fold and 18-fold PQCs by using Rigorous Coupled Wave Analysis (RCWA) [20]. The RCWA algorithm is a rigorous solution of Maxwell's equation with periodic boundary conditions, which is often used to calculate the optical reflection and transmission for various types of photonic structures. The calculated structures are composed of 10 rings of air holes in the dielectric material with refractive index n=1.7. The filling factor is set as r/a=0.2, where r is the radius of the air hole and a=1μm is the lattice constant.

Figure10 indicates their transmittance of TE and TM modes change with the wavelength, respectively. Two complete PBGs are clearly observed when using different polarization modes, TE and TM modes. The 12-fold PQCs show band widths of 0.52 μm (λ=2.42～2.94μm) and 0.241μm (λ=1.337～1.578μm). In consideration of the lattice constant a=1μm, the corresponding frequency widths are 0.073 (a/λ=0.34～0.413) and 0.114 (a/λ=0.634～0.748), respectively. The 18-fold PQCs

show band widths of 0.8μm (2.48～3.28μm) and 0.28μm (1.35～1.63μm) with corresponding frequency widths of 0.1 (a/λ=0.3～0.4) and 0.128 (a/λ=0.613～0.741), respectively. And as for the photonic bandgap in the long wavelength, 18-fold PQCs have deeper transmission peak and less fluctuation than 12-fold structures. From these figures, we can see that PBG characteristic of 18-fold PQCs is better than that of 12-fold PQC. This shows that with the increase of PQC rotational symmetries, the PBG can be improved.

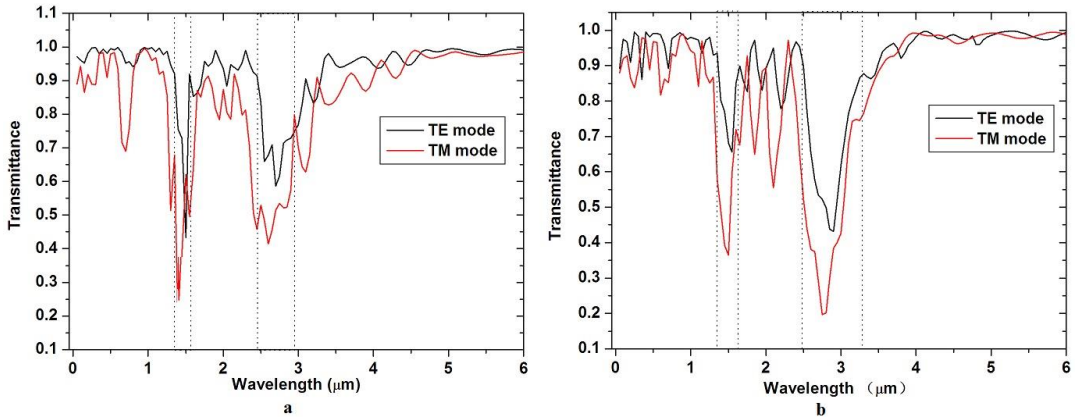

Figure10 Transmittance of a) 12-fold PQC, b) 18-fold PQC

5. Conclusion

We present here a simple fabrication method for complex PQCs by using a single-prism common-path interference. By adjusting the rotation angle as well as controlling the exposure times of photosensitive media, PQCs with complex structures and arbitrary rotational symmetries can be produced in the 2D and 3D space. Multifold PQC patterns are demonstrated using the prism and the TCTP prism system, respectively. A quantitative analysis is also developed to potentially design guidance between PQC symmetry and key process parameters. Photonic band studies on these complex PQCs reveal that the characteristics of photonic band-gaps can be improved with the increase of symmetries. Thus, it can potentially provide new means to develop PQCs with complete bandgaps.

Acknowledgement

This work is supported by the Foundation Research Project of Henan Province

(No. 152300410023) and National Natural Science Foundation of China (No.11104251).

References

[1] Z.V.Vardeny, A.Nahata, A.Agrawal: Optics of photonic quasicrystals, Nature Photonics 7, (review) 177-187, (2013)

[2] M.A.Grado-Caffaro, M.Grado-Caffaro: "On the refractive index of photonic quasicrystals" in Photonic crystals:optical properties,fabrication and applications, Nova Science Pub., W.L.Dahl (Editor), 2011,chapter17,pp.341-344

[3] C.Janot, Quasicrystals: a primer (2nd edition, Oxford University Press, Oxford, 1994)

[4] Rechtsman, M., Jeong, H. C., Chaikin, P., Torquato, S. & Steinhardt, P. Optimized structures for photonic quasicrystals. *Phys. Rev. Lett.* **101,** 073902 (2008).

[5] Kaliteevski, M. A. *et al.* Diffraction and transmission of light in low-refractive index Penrose-tiled photonic quasicrystals. *J. Phys. A* **13,** 10459–10470 (2001).

[6] Zoorob, M. E., Charlton, M. B. D., Parker, G. J., Baumberg, J. J. & Netti, M. C. Complete photonic bandgaps in 12-fold symmetric quasicrystals. *Nature* **404,** 740–743 (2000).

[7] Steurer, W. & Sutter-Widmer, D. Photonic and phononic quasicrystals. *J. Phys. D* **40,** R229–R247 (2007).

[8] Wijnhoven J. E. G. J. and Vos W L, "Preparation of photonic crystals made of air spheres in Titania," Science 281, 802-804 (1998).

[9] Lin S Y, Fleming J G, Hetherington D L, Smith B K, Biswas R, Ho K M, Sigalas M M, Zubrzycki W, Kurtz S R and Bur J, Three-dimensional photonic crystal operating at infrared wavelengths," Nature 394, 251-253 (1998).

[10] Sun H B, Matsuo S M, and Misawa H, "Three-dimensional photonic crystal structures achieved with two-photon-absorption photopolymerization of resin"Appl. Phys. Lett.74, 786 (1999).

[11] Campbell M, Sharp D N , Harrison M T, Denning R G and Turberfield A J, "Fabrication of photonic crystals for the visible spectrum by holographic lithography",

Nature, 404, 53-56 (2000)

[12] Zito G, Piccirillo B, Santamato E, Marino A, Tkachenko V, Abbate G, “Two-dimensional photonic quasicrystals by single beam computer-generated holography", Opt Express.16(8), 5164-5170 (2008).

[13] Wang X, Ng C Y, Tam W Y, Chan C T and Sheng P, “Large-Area Two-Dimensional Mesoscale Quasi-Crystals”, Adv. Mat ., 15, 1526-1528 (2003).

[14]Yang Y, Zhang S H, and Wang G P, “Fabrication of two-dimensional metal-dielectric quasicrystals by single-beam holography”, Appl. Phys. Lett., 88, 2511041-2511043 (2006).

[15]Wu L J, Zhong Y C, Chan C T, and Wong K S, Wang G P, “Fabrication of large area two- and three-dimensional polymer photonic crystals using single refracting prism holographic lithography”, Appl. Phys. Lett., 88, 0911151-0911153 (2006).

[16] Sun X H, Tao X M, Ye T J, Xue P, Szeto Y S, Optical design and fabrication of 3D electrically switchable hexagonal photonic crystal, Appl. Phys. B: Lasers and Optics, 87 (1), 65-69, (2007).

[17] Sun X, Tao X, Ye T, Xue P, Szeto Y S, 2D and 3D electrically switchable hexagonal photonic crystal in the ultraviolet range, Applied Physics B: Lasers and Optics, 87(2), 267-271 (2007).

[18] Sun X H, Tao X M and Wang Y Y, Various photonic crystal structures fabricated by using a top-cut hexagonal prism, Applied Physics A., 98(2), 255-261 (2010).

[19] Sun X H., Liu W, Wang G L, Tao X M, Optics design of a top-cut prism interferometer for holographic photonic quasi-crystals, Optics Communications, 285, 4593-4598 (2012).

[20] Moharam M G, Pommet D A, and Grann E B, Stable implementation of the rigorous coupled-wave analysis for surface-relief gratings enhanced transmittance matrix approach, J. Opt. Soc. Am. A., 12, 1077-1086 (1995).